2020 IEEE/RSJ International Conference on Intelligent Robots and Systems (IROS)
October 25-29, 2020, Las Vegas, NV, USA (Virtual)

Goal-driven variable admittance control for robot manual guidance

Davide Bazzi[1], Miriam Lapertosa[1], Andrea Maria Zanchettin[1] and Paolo Rocco[1]

Abstract— **In this paper we address variable admittance control for human-robot physical interaction in manual guidance applications. In the proposed solution, the parameters of the admittance filter can change not only as a function of the current state of motion (i.e. whether the human guiding the robot ia accelerating or decelerating) but also with reference to a predefined goal position. The human is in fact gently guided towards the goal along some curved paths, where the damping is conveniently scaled in order to accommodate the motion towards the goal position. The algorithm also allows the human to reach goals that he/she cannot directly see because for example the transported object is bulky and obstructs the worker view. The performance of the proposed controller are evaluated by means of point to point cooperative motions with multiple volunteers using an ABB IRB140 robot.**

I. Introduction

Robots have been used in industry and studied in research since many years. The majority of the considered cases are related to situations where the robot repeats cyclically the same operations, with high speed and precision. Moreover, for safety reasons, the robots are segregated into cells inside which the human is not allowed to enter, unless all the robots are stopped. In the last decade, collaborative robotics has raised a lot of interest, since it allows to combine the best capabilities of the robots with those of the human. Speed and quality of the industrial processes and the health of the worker can be improved, reducing his/her fatigue and alienation. This scenario brings new challenges and safety issues because human and robot work together in the same space without a physical barrier that guarantees the operator safety. Even though collaborative robotics brings an increase of complexity, it is of great value because in many situations it is desirable to mix the force, speed, accuracy typical of a robot with the human intelligence and manual skills.

Hand-guiding of robots is another collaborative operation allowed by safety standards. A typical application is the handling of large and heavy loads that human cannot lift up by himself[1]. A robot compensates for the gravitational and inertial load of the transported object while a human simply guides the robot end-effector to the right place (one of the predefined goals). In these applications, a force-torque sensor can be mounted on the robot end-effector in order to measure the applied operator force and estimate his intention of motion. To make the robot compliant with the force applied by the human, an admittance control is typically implemented on the machine. This technique simply converts the human force into a speed or position reference for the robot end-effector that is then managed by the low level position and velocity axis control of the robot. The aforementioned conversion is realized by the so called admittance filter that enforces a mass-spring-damper dynamics when a human applies a force at the end-effector. In human-guidance applications, the stiffness term is usually not needed because a desired equilibrium position is not set: therefore only the mass and damping parameters are of interest.

Linear, fixed-gain admittance filters, however, entail a trade-off in the achievable performance: indeed, small parameters help in fast motions with low precision and low human-effort, while large ones allow precise motion but slow movements and high operator fatigue. Obviously, it is desirable that the control law exhibits the appropriate behaviour depending on the working condition. For this reason, several researchers have proposed different algorithms under the name of variable impedance/admittance control in which they try to estimate the human will of motion and change the parameters accordingly. The underlying idea consists in reducing both the mass and the damping in case of acceleration, decreasing damping in case of cruise speed and reducing mass while increasing damping in case of deceleration. Ikeura et al. [1] presented a very simple variable admittance control consisting in two different invariable admittance controls, one for low velocity and the other one for medium and high speed. In [2], the authors assume to model the human arm as a pure damper and then they fit the parameters of the model by means of a recursive least square procedure. The estimated relation is used as an admittance control for the robot. [3] divided the operation in four subsequent situations by means of some thresholds. Inside each working section, they applied specific dynamic parameters between the minimum, maximum and nominal values in order to have continuous transitions. In [4], the authors focused on low velocity situations and approximate the human impedance just to a spring. Then, they online estimate the stiffness of the human arm and impose that the damping of the robot for slow motion is proportional to it. Duchaine et al. [5] proposed a law that varies the damping proportionally to the derivative of the force applied by the human, projected along the speed of the end-effector. In [6] the human will to accelerate or decelerate was first estimated by comparing the acceleration and speed signs. The damping parameter was varied proportionally to the

This work was supported by the Smart4CPPS project funded by Regione Lombardia (Accordi per la Ricerca e l'Innovazione, Grant ID 236789).

[1] The authors are with Politecnico di Milano, Dipartimento di Elettronica, Informazione e Bioingegneria, Piazza L. Da Vinci 32, 20133, Milano, Italy (e-mail: {davide.bazzi, andreamaria.zanchettin, paolo.rocco}@polimi.it, miriam.lapertosa@mail.polimi.it).

[1]Here and in the following, when referring to the human operator, "he" has to be intended as "he/she".

acceleration module. The mass parameter was changed in order to keep constant the bandwidth of the admittance filter which is more intuitive for the operator. The topic of variable admittance control has been also faced by some more recent work by means of machine learning techniques [7], [8]. The objective was to find the best set of parameters for a specific person in order to realise a predefined linear path. In [9], the authors use a multilayer feed-forward neural network that established the damping value in response to a certain end-effector velocity and to a human force.

All these and other works [10], [11], [12], [13], [14], [15], [16] are focused on varying the admittance parameters according to the intensity of the human force and velocity and their relative directions in order to understand if the human wants to accelerate, travel at constant speed or decelerate.

The variation of the parameters according to the direction of the force is instead unexplored. This latter dependency could be obviously very useful if the human wants to, or has to, reach a precise known goal position. As a matter of fact, with the existing solutions the problem of directing towards a specific goal has always been in charge to the human. This can be a challenging task if the transported object has a big inertia and/or has big size that blocks the view of the target position to the human.

In this paper, we introduce a new physical interpretation of the admittance filter that extends the classical one. This allows to realize variable admittance filters that not only permit to overcome the classical trade-off of the invariable admittance filter as done in many ways in literature but it also ensures to actively assist the human in directing towards a goal position also along non linear paths (up to now the majority of the proposed algorithms look at linear paths).

The rest of the paper is organized as follows. Section II introduces a new extended physical interpretation of the admittance filter and in particular of the dependency of its parameters also on the human force direction and on the relative position of the end-effector with respect to the goal. In Section III, a variable admittance control that actively helps the human in redirecting towards the predefined goal is presented, based on the new interpretation. Then, some improvements and extensions of the proposed strategy are described. In Section IV, different kinds of experiments are conducted in order to verify the goodness of the presented approach. In the end, some conclusions are drawn.

II. A NEW INTERPRETATION OF THE ADMITTANCE FILTER

Consider a one-dimensional admittance filter without the elastic term:

$$v = \frac{1}{ms + d} f \tag{1}$$

where m and d respectively represent the virtual mass and damping that the human perceives when applying a force f at the end-effector and v is the speed reference for the robot tool frame.

The relation (1) can be extended to the general 3-dimensional case adopting an admittance filter for each component of the force in a decoupled fashion:

$$\begin{aligned} v_x &= \tfrac{1}{m_x s + d_x} f_x \\ v_y &= \tfrac{1}{m_y s + d_y} f_y \\ v_z &= \tfrac{1}{m_z s + d_z} f_z \end{aligned} \tag{2}$$

where v_x, v_y, v_z are the Cartesian components of speed vector $\boldsymbol{v}$ and f_x, f_y, f_z the ones of the applied force $\boldsymbol{f}$.

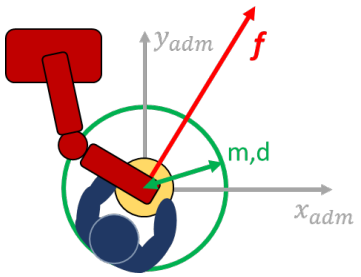

Fig. 1: Pictorial view of the space dependence of the admittance parameters in invariable admittance control.

As reported in the literature, the parameters of the three filters should be selected equal in order to preserve a natural engagement between human and robot. Therefore, the relationship between force and velocity in 3-dimensional space can be written as follows:

$$\boldsymbol{v} = \frac{1}{ms + d} \boldsymbol{f} \tag{3}$$

If the force $\boldsymbol{f}$ applied by the human has a constant or slowly varying direction in time, then filter (3) does not change such direction, i.e. the velocity vector will have the same direction as the force, with filtered amplitude.

The extended interpretation of the admittance filter that will be discussed in the following consists in modelling each parameter as possibly dependent on the spatial direction of the human force. With this in mind, each parameter of a classical invariant admittance filter can be associated in 3-dimensional space to a sphere with radius equal to its constant value and centred in the origin of a frame defined at the robot end-effector with axes parallel to the global frame, see Fig.1. In all the variable admittance control techniques proposed in literature each parameter is varied according to a scalar function depending on the intensity of the force, acceleration and/or velocity or on some estimates of the stiffness or damping of a human arm. In our graphical interpretation, this is equivalent to modulating the radius of the sphere, without any directional information.

Suppose now that a goal position $\boldsymbol{p_G}$ has been defined, i.e. a position that the end-effector of the robot, hand-guided by the human, is supposed to approach. The idea is to modulate the gains of the admittance filter (3) accounting for such goal position $\boldsymbol{p_G}$, in such a way to make the human more comfortable when moving towards the goal, without however constraining the motion on an assigned path. Coming back to our geometrical interpretation, a 3D shape has to be introduced, that depends on the relative orientation of the

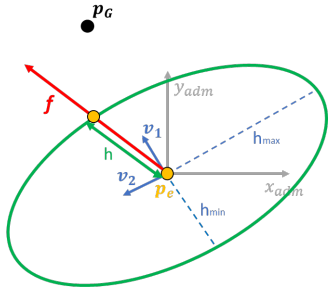

Fig. 2: Representation of the ellipsoid that defines the parameters space dependency.

applied force and the direction towards the goal position. The parameters of such 3D volume will be used to suitably modulate the gains of the admittance filter as explained in the next Section.

III. Developed Strategy

The proposed strategy consists in assigning to each parameter of the admittance filter an appropriate dependency on the human force direction as a function of the relative position of the predefined goal with respect to the actual robot end-effector. In order to do so, it is necessary to shape the parameter space dependency rather than with a sphere with a different shape, constructed based on the desired target. In particular, we have used an ellipsoid that has the first principal axis pointing from the actual end-effector position to the goal one, the second principal axis normal to the first one and belonging to the horizontal plane passing through the interaction point, while the third one completes a right hand frame. The length of the first principal semi-axis is chosen equal to the minimum value for that parameter while to the other two semi-axes the maximum value of the parameter is assigned. Then, the value of a parameter at a certain time instant is equal to the distance between the centre of the ellipsoid and the point given by the intersection between this shape and the line containing the force vector.

Consider Fig.2: first of all, remember that the ellipsoid will be expressed in a frame centred in the end-effector position and oriented as the global frame. An ellipsoid centred in the origin can be expressed just through a 3×3 positive definite matrix $\boldsymbol{A}$ since it is defined as the set of points $\boldsymbol{x} \in \mathbb{R}^3$ that satisfy the following equation:

$$\boldsymbol{x}^\top \boldsymbol{A}\, \boldsymbol{x} = 1 \tag{4}$$

The eigenvectors $\boldsymbol{v_i}$, $i = 1, 2, 3$, of $\boldsymbol{A}$ define the principal axes of the ellipsoid and therefore, according to the previously described strategy, they are computed in the following way:

$$\begin{aligned} \boldsymbol{v_1} &= \frac{\boldsymbol{p_G} - \boldsymbol{p_e}}{\|\boldsymbol{p_G} - \boldsymbol{p_e}\|} \\ \boldsymbol{v_2} &= \frac{\boldsymbol{z} \times \boldsymbol{v_1}}{\|\boldsymbol{z} \times \boldsymbol{v_1}\|} \\ \boldsymbol{v_3} &= \boldsymbol{v_1} \times \boldsymbol{v_2} \end{aligned} \tag{5}$$

where $\boldsymbol{p_G}$ is the absolute goal position, $\boldsymbol{p_e}$ is the end-effector position and $\boldsymbol{z}$ is the unit vector in the direction of the z-axis of the frame in which the ellipsoid is defined (which is oriented as the global frame). Then, the eigenvectors can be arranged in a 3×3 matrix $\boldsymbol{Q}$:

$$\boldsymbol{Q} = [\boldsymbol{v_1} | \boldsymbol{v_2} | \boldsymbol{v_3}] \tag{6}$$

Matrix $\boldsymbol{Q}$ also expresses the orientation of the ellipsoid principal axes frame with respect to the frame in which we have chosen to define it. Being a rotation matrix, $\boldsymbol{Q}$ is an orthogonal matrix, i.e. its inverse is equal to its transpose. The eigenvalues λ_i, $i = 1, 2, 3$, of $\boldsymbol{A}$ are the reciprocals of the squares of the semi-axes length. Therefore, for the generic parameter h (the mass or the damping factor) that has minimum value h_{min} and maximum one h_{max}, the associated eigenvalues are selected as:

$$\begin{aligned} \lambda_1 &= \frac{1}{(h_{min})^2} \\ \lambda_2 &= \frac{1}{(h_{max})^2} \\ \lambda_3 &= \frac{1}{(h_{max})^2} \end{aligned} \tag{7}$$

The eigenvalues can be collected inside a 3×3 diagonal matrix $\boldsymbol{\Lambda_h}$. Then, the matrix $\boldsymbol{A_h}$ representing the ellipsoid for the generic parameter h is obtained as:

$$\boldsymbol{A_h} = \boldsymbol{Q} \boldsymbol{\Lambda_h} \boldsymbol{Q}^{-1} = \boldsymbol{Q} \boldsymbol{\Lambda_h} \boldsymbol{Q}^\top \tag{8}$$

In particular, we will have the mass ellipsoid $\boldsymbol{A_m}$ and the damping ellipsoid $\boldsymbol{A_d}$ associated to the minimum and maximum values of the mass and the damping, respectively. The value of the generic parameter h is computed as the distance from the centre of the ellipsoid to one of the two points found as the intersection of this shape with a straight line directed as the human force vector $\boldsymbol{f}$. Such a value can be found through the following formula:

$$h = \frac{1}{\sqrt{\boldsymbol{u_f}^\top \boldsymbol{A_h} \boldsymbol{u_f}}} \tag{9}$$

where $\boldsymbol{u_f}$ is a unit vector in the same direction of the force $\boldsymbol{f}$.

Moreover, as it has already been mentioned, it is simple to integrate whatever variable admittance strategy proposed in literature in the one previously described. Indeed, it is possible to apply to the result (9) of our algorithm another transformation that takes into account the scaling of the parameters based on acceleration, cruise speed and deceleration states. In our interpretation, this would entail an ellipsoid that not only changes its axes orientation in time but also its axes length according to a common time-varying scaling coefficient. In the following, we will describe two improvements of the strategy previously described.

A. Damping Ellipsoid

As it is well known in literature, a low mass is always desirable both in acceleration (human force pointing to the goal) and deceleration (human force pointing in opposite direction to the goal). This behaviour is guaranteed by the symmetric structure of the ellipsoid. Instead, a low damping is advisable when the human is pushing towards the target

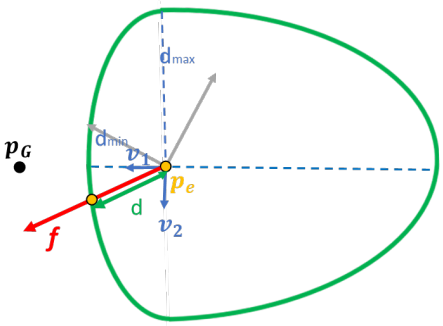

Fig. 3: Representation of the improved shape for the damping constituted by the union of two half-ellipsoids.

while a high damping is convenient when the worker is pulling the robot in order to brake it in proximity of the goal position because it helps to slow down the manipulator. This desired feature is not realised by the damping ellipsoid previously defined. Consider then Fig.3: the idea is to assign a different shape to the damping in the two half-spaces in which the working region is divided by the plane described by the second and the third principal axes. A possible approach is to combine two half-ellipsoids in correspondence of the aforementioned plane. The first one is the half of the ellipsoid described in Section III that belongs to the half-space containing the target. The second half is characterized by the same principal axes directions and the only difference is the length of the first semi-axis that is chosen greater or equal to the maximum value for that parameter. In this way, an asymmetric spatial shape is given to the damping that reflects the desired feature. Notice that:

- what we have called maximum value is actually a value that we chose for the length of the second and third semi-axes and it is not a physical or a realisation limitation. Indeed, as reported many times in the literature, there are no limitations for the maximum values that can be assigned to mass and damping parameter. Therefore, it is not surprising that the length of the first principal semi-axis length of the second half-ellipsoid can be chosen greater than the value that we have called maximum value.
- The combination of the two half-ellipsoids does not create any discontinuity in the overall shape assigned to the damping.

B. Ellipsoid first principal axis direction

In Section III we proposed that the first principal axis of the ellipsoid was directed as the vector that connects the actual end-effector position to the goal one. However, this might be not the best solution if for some reason the actual speed is not pointing to the target, namely if the path that the human will follow to reach the goal won't be linear but curved. In such a case, the choice we previously made would induce an additional effort for the human because, in order to change the speed direction, he/she applies a continuous directional force profile that cannot be instantaneously directed along $\boldsymbol{v_1}$. The previous choice of $\boldsymbol{v_1}$ would then entail a high

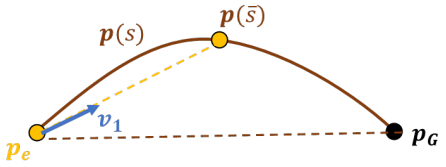

Fig. 4: Representation of the minimum curvature path and of the new ellipsoid first semi-axis direction.

damping value that causes a large human effort. Therefore, it is better if the human is progressively redirected to the target along a curve in a smooth way avoiding in this way to cause him an additional effort. For this purpose, the direction for the first principal axis will be determined according to the following steps, making reference to Fig.4:

1) The minimum curvature path $\boldsymbol{p}(s)$ in the normalized path coordinate s that connects the actual position to the goal one satisfying the actual velocity is computed at each time instant k. More precisely, $\boldsymbol{p}(s)$ is selected with a polynomial structure of the 4^{th}-order and has to minimize the curvature of the line satisfying the following bounds:

$$\begin{array}{ll} \boldsymbol{p}(0) = \boldsymbol{p_e}(k) & \boldsymbol{p}(1) = \boldsymbol{p_G} \\ \boldsymbol{p}'(0) = \boldsymbol{v_e}(k) & \boldsymbol{p}'(1) = \boldsymbol{0} \end{array} \tag{10}$$

where $\boldsymbol{p}'(s)$ indicates the first derivative of the path $\boldsymbol{p}(s)$ with respect to s, $\boldsymbol{p_e}(k)$ and $\boldsymbol{v_e}(k)$ are respectively the actual position and speed of the end-effector, $\boldsymbol{p_G}$ is the goal position.

2) Then, a point $\boldsymbol{p}(\bar{s})$ belonging to the computed curve at the $\bar{s} \in [0, 1]$ of its completion is considered. The ellipsoid first principal axis direction $\boldsymbol{v_1}$ is selected as:

$$\boldsymbol{v_1} = \frac{\boldsymbol{p}(\bar{s}) - \boldsymbol{p_e}}{\|\boldsymbol{p}(\bar{s}) - \boldsymbol{p_e}\|} \tag{11}$$

while $\boldsymbol{v_2}$ and $\boldsymbol{v_3}$ are computed as in (5). If $\bar{s}$ is chosen equal to 1, then $\boldsymbol{v_1}$ becomes again equal to (5) and therefore this minimum curvature approach can be seen as an additional generalization to the first proposed strategy. Instead, if $\bar{s}$ is chosen equal to 0, then the first axis is directed as the actual speed and this would entail that the goal is not considered. In this case, the strategy would completely accommodate whatever motion the robot is doing. So, no help in redirecting to the desired target would be given to the human if $\bar{s} = 0$. Therefore, a proper value for $\bar{s}$ has to be selected between the two extremes in order to help the human in a smoother way with respect to the first strategy presented in section III. Consider that usually it is desirable to have grater motion freedom ($\bar{s} = 0$) at the beginning of the movement while a more precise and constrained motion ($\bar{s} = 1$) at the end of the path while the human is approaching the goal position. Therefore, we have decided not to select a fixed value for $\bar{s}$, rather to change it according to the following equation:

$$\bar{s} = 1 - e^{-\frac{\|\boldsymbol{p_e} - \boldsymbol{p_0}\|}{\|\boldsymbol{p_e} - \boldsymbol{p_G}\|}} \tag{12}$$

where $\boldsymbol{p_e}$ is the actual end-effector position, $\boldsymbol{p_G}$ is the goal position and $\boldsymbol{p_0}$ is the starting point of the whole motion. Equation (12) guarantees to have both freedom of motion ($\bar{s} = 0$) in proximity of the starting point and an accurate motion ($\bar{s} = 1$) around the target location.

Notice that this procedure generalizes the first proposed strategy for the selection of the ellipsoid first principal axis in case of curved path. Indeed, if the speed is perfectly directed towards the goal, then this direction coincides with the one determined by the first strategy.

IV. Experimental results

The experimental validation of the algorithm described in this paper is divided in two parts. In the first one, the developed approach is compared with three invariable admittance controls having the same bandwidth but with different damping value (small, medium and high). The reason under which the developed technique is compared with constant admittance filters instead of another variable admittance strategy in literature is that the proposed algorithm can be applied jointly with whatever constant or variable admittance filter in literature. Therefore, in order to only highlight the contributions of the presented method, in the experimental results section the described strategy is superimposed to a constant admittance filter and not to a variable one. The objective of this first part of the validation phase is to reach a pre-determined marked goal position as quickly as possible and with the best possible accuracy. The target position is selected in a way that is impossible to be reached from the starting point along a linear path. The obtained results will be analysed in terms of completion time, positioning precision, path length and required human energy.

In the second experimental part, we ask the worker to reach a random goal position that we have selected inside the robot operating space. The human does not know where the goal is, since the target is not marked in this case. In the latter experiment we want to show that the proposed approach returns to the worker a natural and intuitive directional feedback that allows him to reach, with a certain precision, also a goal that he cannot directly see for example due to the size of the carried load.

In the experiments, an ABB IRB140 robot with a Robotiq force/torque sensor mounted on its end-effector is adopted. The worker interacts with the robot through an handle attached to the force sensor. This support maintains its orientation during the movement since in this paper we focus on the translational part only of the motion. In particular, the human applies a force at the handle and the manipulator moves in the 3-dimensional Cartesian workspace according to the corresponding end-effector speed reference generated by the admittance filter, which are then converted in joints position and velocity references. The robot is already equipped with a position and speed controller for each joint, whose sampling time is 4 ms.

Moreover, due to the difficulty in indicating the target and evaluating the performance in case of a 3-dimensional goal position, we have set as a target a point in the horizontal plane independent of the height of the end-effector. Therefore, the target can be seen as a vertical line passing through a desired point in any horizontal plane. In order to mark the goal position, we have signed the corresponding point on the ground. Then, a laser pointing downward is mounted on the extreme of the handle with the purpose of facilitating the human comprehension of the actual end-effector position with respect to the target, avoiding errors due to some personal perspective. The experimental set-up is shown in Fig.5.

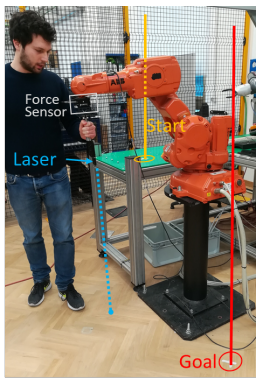

Fig. 5: Picture of the experimental set-up for the first type of experiments.

In order to be consistent with the aforementioned experimental set-up, we have decided to adopt an invariable admittance filter with constant parameters along the z-axis in all the experiments while applying different techniques in the horizontal plane. Therefore, in place of the described ellipsoid in the 3-dimensional workspace, we will have an ellipse in the horizontal plane.

We also consider the stability of the described system and we found empirically that in correspondence of the minimum value used for the mass, $10kg$, the lowest possible value for the damping in order to avoid robot oscillations in case of highly stiff human arm is equal to $100Ns/m$.

A. Performance comparison with invariable admittance filters for curved path

In this set of experiments, each subject (10 in total) is asked to move the robot from the starting position to the target one 5 times with the objective of being as quick as possible during the motion and as accurate as they can in reaching exactly the goal position. Each of them tries all the following four techniques in a random order:

1) Invariable Admittance Filter with low damping (IAF-L): $d = 100Ns/m; m = 10kg$;
2) Invariable Admittance Filter with medium damping (IAF-M): $d = 250Ns/m; m = 25kg$;
3) Invariable Admittance Filter with high damping (IAF-H): $d = 400Ns/m; m = 40kg$;
4) Variable Admittance Filter (VAF) with damping computed as described in the paper with all the presented improvements while the mass is chosen so as to keep

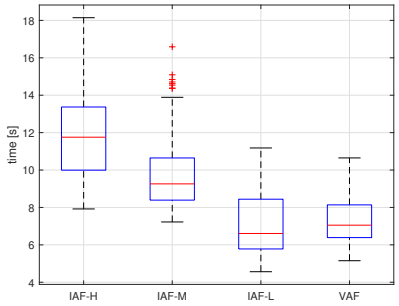

Fig. 6: Statistics of the time needed to complete the path with the different control techniques.

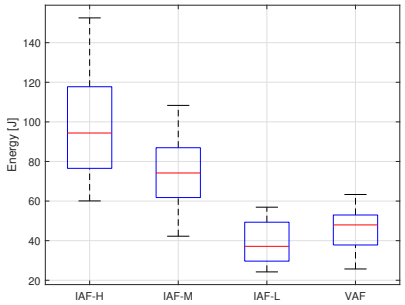

Fig. 7: Statistics of the energy needed to complete the path with the different control techniques.

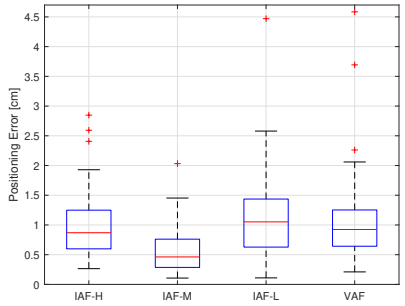

Fig. 8: Statistics of the positioning precision with the different control techniques.

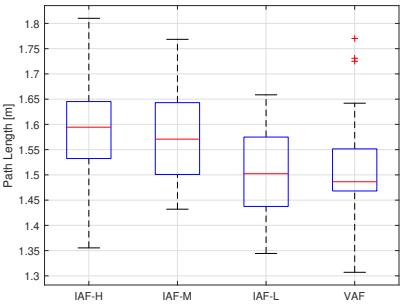

Fig. 9: Statistics of the path with the different control techniques.

at $10rad/s$ the bandwidth of the filter in order to have a more intuitive collaboration.

Before the experiments, each volunteer tries the IAF-M technique for two minutes in order to increase his confidence with the robot. During this period, the subject can conduct the robot where he wants and he is not informed of the tests that he will be asked to do.

As it can be noticed in Fig.5, the target position cannot be reached through a linear path from the starting point because of the presence of the robot structure. This forces the volunteer to approach a curved path towards the target.

As it can be seen from Fig.6, in order to complete the path with VAF it is only necessary a 5% more time than IAF-L, but the variability of the results is lower due to the ability of VAF to help human in approaching the goal position. Instead, VAF takes almost 30% and 70% less time of the IAF-M and IAF-H respectively. An analogous comparison can be done about the human energy required to complete the path, see Fig.(7). VAF requires to the human a small additional effort with respect to IAF-L, while it is much less demanding with respect to IAF-M and IAF-H. In Fig.(8), the positioning error performance are shown. Even though the results are quite similar and good (less than $1cm$ in mean) for the different techniques, VAF guarantees a higher precision than IAF-L and almost equal to the one of IAF-M. Another interesting performance is depicted in Fig.(9). VAF allows the human to complete the task along a shorter path than all the others techniques thanks to its ability of redirecting the human towards the goal. Another interesting feature that emerges looking at the performances of IAF techniques in this plot is that the higher the inertia is (it is proportional to the damping) the longer the path is because it is more difficult to change the speed direction of the moving object. This justifies the need of VAF in order to help the human in redirecting towards the desired target.

In Fig.10, in the sub-figure on the top, the behaviour of the damping parameter on a normalized time scale is shown for the analysed techniques, while in the bottom one a zoom of the final part of the plot is shown. IAF-L, IAF-M, IAM-H are represented with the green, magenta, red solid lines, respectively, while VAF mean value with the blue one. The dashed blue lines indicate the 75^{th} and 25^{th} percentile of VAF damping. At the beginning of the path, the operator cannot go straight to the path due to the already explained reasons and therefore the damping of VAF cannot be at the minimum value. After the 30% of the time the damping starts to settle at the minimum value and also the corresponding percentiles define a smaller bandwidth around the mean value. Then, VAF damping remains at the minimum value for a 55% of the time until the end of the path, when the human has to brake in correspondence of the goal. Indeed in this latter phase, as can be seen in the bottom sub-figure, the VAF mean value almost reaches the maximum damping. Another interesting thing to notice from Fig.10 is that with VAF the human is guiding the robot straight towards the path just after the 30% of the trajectory time. This can be understood observing that after the first 30% of time, the damping takes the minimum value, that means the human is

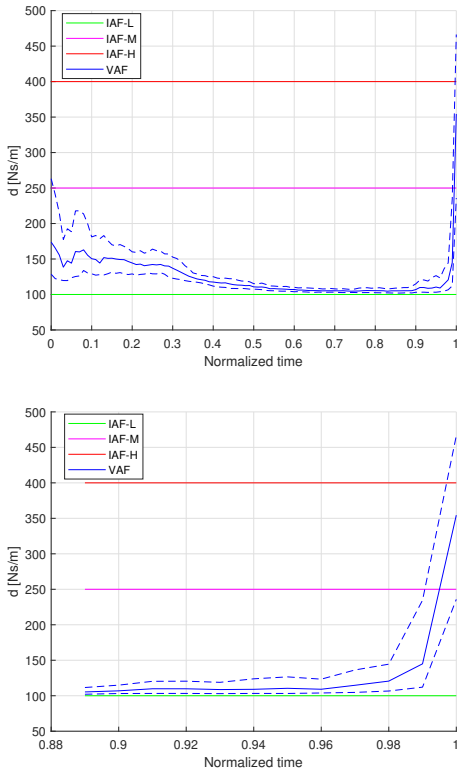

Fig. 10: Behaviour on a normalized time scale of the virtual damping for the different control tecniques: IAF-L in solid green line, IAF-M in solid magenta line, IAF-H in solid red line, VAF in solid blue line while in dashed blue lines the 75^{th} and 25^{th} percentile of VAF.

moving straight to the target.

After this set of experiments, the volunteers are asked to answer two questions in order to compare their experience using the four different techniques, see Fig.11. This plot shows relative results between VAF and the IAF techniques. VAF requires less than 20% additional effort with respect to IAF-L, but it is more than 20% easy in approaching the goal. Instead, VAF requires 80% and 50% less energy than IAF-H and IAF-M respectively while VAF is less precise by 40% and 30% than IAF-H and IAF-M. Therefore, VAF is globally better than IAF-H and IAF-M.

B. Random unknown goal

In this set of experiments, each volunteer is asked to move the robot from the usual starting position to an unknown target that has been randomly selected inside the robot operating space. In particular, the human has only 40 seconds at his disposal in order to approach the goal position as accurate as he can. In the latter set of experiments we want to show that the proposed approach returns to the worker a natural and intuitive directional feedback that allows him to reach, with a certain precision, also a goal that he cannot directly see for example due to the size of the transported load. The volunteer will use only our proposed technique to accomplish this task since the other strategies do not distinguish between space directions and therefore they will

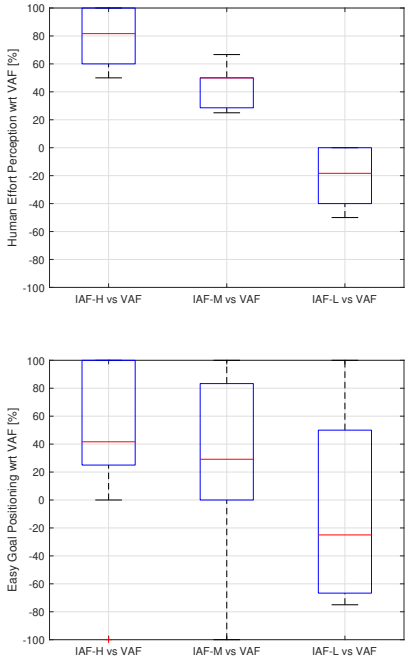

Fig. 11: Questionnaire statistics of the effort and the easy of approaching the goal position of the invariant control techniques with respect to the variable strategy. The relative results are expressed in percentage.

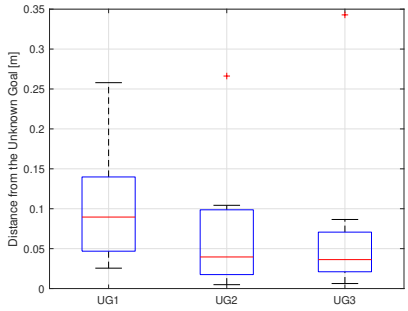

Fig. 12: Statistics of the positioning precision in reaching the subsequent unknown random goal position.

fail in this type of task. Each volunteer is asked to reach 3 different randomly chosen goals as accurately as they can with only one shoot for each goal. The statistics about the distance of the final position from the unknown goal are reported in Fig.12 divided in the 3 subsequent unknown goals. It is clear that with practise the performance increases: indeed both the mean value and the difference in the subject results decrease. Even though the volunteers have never tried such a task before and have no experience with physical interaction with a robot, the obtained results are very good. Indeed, at the first trial the mean error is already under $10cm$ and at the third one is under $4cm$ with low variability.

At the end of this set of experiments volunteers are asked to answer four questions evaluating their experience with a mark from 1 to 10:

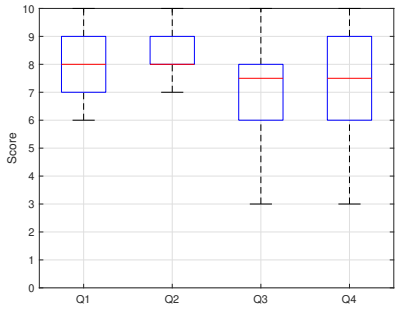

Fig. 13: Questionnaire statistics about the unknown goal approaching experience.

- Q1 is about ease of perception of the right direction in which the subject should guide the robot;
- Q2 is about the possibility of improving the performance with more practise;
- Q3 asks if they clearly perceive to be in proximity of the target;
- Q4 asks about their confidence in having reached the unknown goal position with a good precision.

The results are shown in Fig.13. The volunteers argue that it was easy to perceive the right motion direction and that with some additional practise the performance surely increase. Moreover, they state that they clearly understand of being near to the goal position and therefore they are confident that they have reached the target with a good accuracy.

V. Conclusion

In this paper, a novel extended physical interpretation of the classical admittance control in human-robot physical interaction is proposed. The admittance parameters are made dependent also on the relative direction between the force and the relative position of the goal with respect to the actual position. Based on this new idea, we have conceived a variable admittance control that enriches the classical algorithms with the ability to help the human in directing towards a predefined goal position also along a curved path. The idea is to modulate the damping so that the human perceives a higher resistance in the wrong directions and a lower one in the correct direction. Moreover, it allows to reach target positions even in case the human cannot directly see the goal because for example the transported object is bulky and obstructs the worker view. This is possible thanks to the intuitive and natural feedback that this strategy returns to the human operator. The performance of the proposed controller are evaluated by means of point to point cooperative motions with 10 volunteers and compared with the ones of three constant damping controllers in terms of: human energy, completion time, positioning error and path length. The results show that the proposed strategy is the best compromise since it combines the positive aspects of the constant law damping and constant high damping controls. Then, the ability of approaching completely unknown goals is tested and successfully validated.

The proposed control technique constitutes the first fundamental step towards a multi-goal scenario, where human can arbitrarily decide where to guide the robot among a predefined set of goals.

References

[1] R. Ikeura and H. Inooka, "Variable impedance control of a robot for cooperation with a human," in *Proceedings of 1995 IEEE International Conference on Robotics and Automation*, vol. 3, May 1995, pp. 3097–3102 vol.3.

[2] R. Ikeura, T. Moriguchi, and K. Mizutani, "Optimal variable impedance control for a robot and its application to lifting an object with a human," in *Proceedings. 11th IEEE International Workshop on Robot and Human Interactive Communication*, Sep. 2002, pp. 500–505.

[3] T. Tsumugiwa, R. Yokogawa, and K. Hara, "Variable impedance control with regard to working process for man-machine cooperation-work system," in *Proceedings 2001 IEEE/RSJ International Conference on Intelligent Robots and Systems. Expanding the Societal Role of Robotics in the the Next Millennium (Cat. No.01CH37180)*, vol. 3, Oct 2001, pp. 1564–1569 vol.3.

[4] ——, "Variable impedance control based on estimation of human arm stiffness for human-robot cooperative calligraphic task," in *Proceedings 2002 IEEE International Conference on Robotics and Automation (Cat. No.02CH37292)*, vol. 1, May 2002, pp. 644–650 vol.1.

[5] V. Duchaine and C. M. Gosselin, "General model of human-robot cooperation using a novel velocity based variable impedance control," in *Second Joint EuroHaptics Conference and Symposium on Haptic Interfaces for Virtual Environment and Teleoperator Systems (WHC'07)*, March 2007, pp. 446–451.

[6] A. Lecours, B. Mayer-St-Onge, and C. Gosselin, "Variable admittance control of a four-degree-of-freedom intelligent assist device," in *2012 IEEE International Conference on Robotics and Automation*, May 2012, pp. 3903–3908.

[7] F. Dimeas and N. Aspragathos, "Reinforcement learning of variable admittance control for human-robot co-manipulation," in *2015 IEEE/RSJ International Conference on Intelligent Robots and Systems (IROS)*, Sep. 2015, pp. 1011–1016.

[8] ——, "Fuzzy learning variable admittance control for human-robot cooperation," in *2014 IEEE/RSJ International Conference on Intelligent Robots and Systems*, Sep. 2014, pp. 4770–4775.

[9] A. Sharkawy, P. N. Koustournpardis, and N. Aspragathos, "Variable admittance control for human-robot collaboration based on online neural network training," in *2018 IEEE/RSJ International Conference on Intelligent Robots and Systems (IROS)*, Oct 2018, pp. 1334–1339.

[10] F. Ficuciello, L. Villani, and B. Siciliano, "Variable impedance control of redundant manipulators for intuitive human–robot physical interaction," *IEEE Transactions on Robotics*, vol. 31, no. 4, pp. 850–863, Aug 2015.

[11] V. Duchaine, B. Mayer St-Onge, D. Gao, and C. Gosselin, "Stable and intuitive control of an intelligent assist device," *IEEE Transactions on Haptics*, vol. 5, no. 2, pp. 148–159, April 2012.

[12] I. Ranatunga, S. Cremer, D. O. Popa, and F. L. Lewis, "Intent aware adaptive admittance control for physical human-robot interaction," in *2015 IEEE International Conference on Robotics and Automation (ICRA)*, May 2015, pp. 5635–5640.

[13] F. Dimeas and N. Aspragathos, "Online stability in human-robot cooperation with admittance control," *IEEE Transactions on Haptics*, vol. 9, no. 2, pp. 267–278, April 2016.

[14] M. S. Erden and T. Tomiyama, "Human-intent detection and physically interactive control of a robot without force sensors," *IEEE Transactions on Robotics*, vol. 26, no. 2, pp. 370–382, April 2010.

[15] C. T. Landi, F. Ferraguti, L. Sabattini, C. Secchi, M. Bonfè, and C. Fantuzzi, "Variable admittance control preventing undesired oscillating behaviors in physical human-robot interaction," in *2017 IEEE/RSJ International Conference on Intelligent Robots and Systems (IROS)*, Sep. 2017, pp. 3611–3616.

[16] C. T. Landi, F. Ferraguti, L. Sabattini, C. Secchi, and C. Fantuzzi, "Admittance control parameter adaptation for physical human-robot interaction," in *2017 IEEE International Conference on Robotics and Automation (ICRA)*, May 2017, pp. 2911–2916.